

Date of publication xxxx 00, 0000, date of current version xxxx 00, 0000.

Digital Object Identifier 10.1109/ACCESS.2017.Doi Number

Magnetization Loss in HTS Coated Conductor Exposed to Harmonic External Magnetic Fields for Superconducting Rotating Machines

Mohammad Yazdani-Asrami¹, (Member, IEEE), Wenjuan Song², (Member, IEEE), Min Zhang¹, (Member, IEEE), Weijia Yuan¹, (Senior Member, IEEE), and Xiaoze Pei², (Member, IEEE)

¹Department of Electronic and Electrical Engineering, University of Strathclyde, Glasgow, G1 1XW, U.K.

²Department of Electronic & Electrical Engineering, The University of Bath, Bath, BA2 7AY, U.K.

Corresponding author: Dr. Mohammad Yazdani-Asrami (e-mail: mohammad.yazdani-asrami@strath.ac.uk).

This work was partly supported by the UK Engineering and Physical Sciences Research Council EPSRC [EP/S000720/1], and partly by InnovateUK project [UKCG/11030].

ABSTRACT Previous studies on magnetization AC loss of high temperature superconducting (HTS) coated conductors (CCs) taken into account the ideally sinusoidal external magnetic field, or non-sinusoidal by considering only the harmonics in phase with the fundamental component. However, realistically magnetic field often contains harmonics with different phase angles and amplitudes. In this work, magnetization AC loss in HTS CC was studied, considering the phase angle φ of each harmonic; assuming superconductor is subjected to external magnetic field which is distorted by the 3rd and the 5th harmonics. Phase angle of each harmonic was considered in the range of 0 to 2π and amplitude of fundamental magnetic field, was assumed as 10, 20, 50, and 100 mT. Different distortion level of magnetic field was considered too. It is concluded that phase angle of field harmonic has a significant effect on magnetization loss of HTS CCs.

INDEX TERMS External magnetic field, Harmonic phase angle, HTS coated conductor, Magnetization AC loss.

I. INTRODUCTION

LARGE scale power applications of high temperature superconductors (HTS) have attracted tremendous attention in recent decades thanks to their advantages such as high current-carrying capacity, and low losses, for the use in both grid and specially in transportation systems, including rail, marine, and aviation applications [1]-[7]. HTS coated conductors (CCs) in these applications are mostly exposed to external magnetic field, which is ideally expected to be purely sinusoidal [7]-[8]. Magnetic field is intermediary of the energy conversion in most of large-scale power applications such as superconducting rotating electrical machines. The essence of magnetic field in a rotating electric machine could be non-sinusoidal, due to [9]-[12]: 1) coil/winding distribution in the machine stator, 2) manufacturing tolerances in the construction and assembly process, 3) occurrence of mechanical faults, such as bearing wearing, or dynamic and static eccentricity faults. In such cases, the magnetic field would not be purely sinusoidal and thus, will contain harmonics. Such distorted magnetic fields

cause extra losses in different parts of the machine, from core to HTS coils/windings [10]-[14]. It is vital to precisely estimate the magnetization AC loss in HTS CC under nonsinusoidal external magnetic field in order to develop reliable superconducting application, in particular, for sensitive applications such as electric aircrafts or fusion reactors [14].

In [10], authors studied the effect of harmonic amplitude as well as magnetic field dependency of critical current density on harmonic magnetization loss for ReBCO tapes. In [15], authors explored the AC loss in an HTS coil for wind turbine generators experimentally, under different DC field with AC ripples. In [16]-[17], AC loss in HTS strip under nonsinusoidal current and magnetic field was formulized analytically, only considering harmonic amplitude. In [18], authors studied the total AC loss in a Bi-2223/Ag tape by considering a phase shift between sinusoidal magnetic field and sinusoidal transport current. In [19]-[20], AC losses in a circular HTS double pancake coil under three different nonsinusoidal current/magnetic fields, including saw-tooth, triangle, and square waveforms, were

measured and modelled considering the effect of amplitude, orientation angle, and frequency of applied waveforms.

There is a gap in addressing the dependence of magnetization loss in HTS CC on the phase angle of harmonics of external magnetic field in literature [10]-[21]. Our previous study observed a drastic transport AC loss variation when the current harmonic is at different phase angle [22]-[23].

In this work, we carried out comprehensive numerical calculations to investigate the magnetization loss in HTS CC subjected to distorted external magnetic field with the 3rd and the 5th harmonic orders at different phase angles ranging from 0 to 2 π . The amplitude of fundamental magnetic field varies from 10, 20, 50, and 100 mT. The effect of distortion level of different harmonic orders on magnetization loss in HTS CC was also discussed.

II. Modelling method

Numerical calculations were implemented in COMSOL Multiphysics using 2D finite element (FE) approach, by means of H formulation method [24]-[29]. Two independent variables were implemented in the model, $\mathbf{H} = [H_x, H_y]^T$, where H_x and H_y are parallel and perpendicular magnetic fields, respectively. E - J power law, as seen in (1) was used to characterize the nonlinear relation of local electric field E and local current density J in HTS CC [24]-[25]:

$$E/J = (E_0/J_c(B)) (|J/J_c(B)|)^{n-1} \quad (1)$$

Where B is magnetic field, $E_0 = 1 \mu\text{V/cm}$, n is the constant derived from V - I characteristic, and $J_c(B)$ is the critical current density dependence on external magnetic field. Here, a modified Kim model was adopted, as expressed in (2). J_{c0} is the self-field critical current density. The k , α , and B_0 are curve fitting parameters picked up from [30]-[31].

$$J_c(B) = J_{c0} \left(1 + (k^2 B_x^2 + B_y^2) / B_0^2 \right)^{-\alpha} \quad (2)$$

The governing equation is as follows:

$$\partial(\mu_0 \mu_r \mathbf{H}) / \partial t + \nabla \times (\rho \nabla \times \mathbf{H}) = 0 \quad (3)$$

In the model, parallel magnetic field was set to 0, $H_x = 0$; perpendicular magnetic field with harmonic component, $H_y(t)$, has been applied as formulated in (4),

$$H_y(t) = \frac{B_1}{\mu_0} \sin(2\pi ft) + \frac{B_1}{\mu_0} \text{THD}_k \sin(2\pi kft + \varphi_k) \quad (4)$$

In this model, $f = 50$ Hz was considered. THD_k was defined to denote the distortion level of external magnetic field caused by each harmonic component, $\text{THD}_k = B_{hk}/B_1$, where k is the order of magnetic field harmonic, $k = \{3, 5\}$; and $\text{THD}_k = \{0.02, 0.05, 0.1, 0.15, \text{ and } 0.2\}$ were considered in this paper, i.e. $\text{THD}_k \% = \{2, 5, 10, 15, \text{ and } 20\} \%$. B_{hk} is amplitude of each harmonic magnetic field and B_1 represents the amplitude of fundamental external magnetic field; here, $B_1 = \{10, 20, 50, \text{ and } 100\}$ mT. It is worthwhile to mention that the phase angle φ_k of each magnetic field harmonic varies from 0 to 2 π (i.e., 0 $^\circ$ to 360 $^\circ$), here $k = \{3, 5\}$. The effect of phase angle of harmonic on magnetization AC losses was characterized by every 10

degrees, i.e. $\varphi_k = \{0 : 10^\circ : 360^\circ\}$.

TABLE I
SPECIFICATIONS OF HTS COATED CONDUCTOR

Parameter	Value
Manufacturer	SuperPower
Thickness of superconducting layer (t_{sc}), μm	1
Width of tape (w_{tape}), mm	4
Thickness of tape (t_{tape}), mm	0.095
Critical current (I_{c0}) @ 77K, A	86
E - J power law factor (n)	30
Characteristic electric field (E_0) @ 77K, $\mu\text{V/cm}$	1
Stabilizer material	Copper
Substrate material	Hastelloy

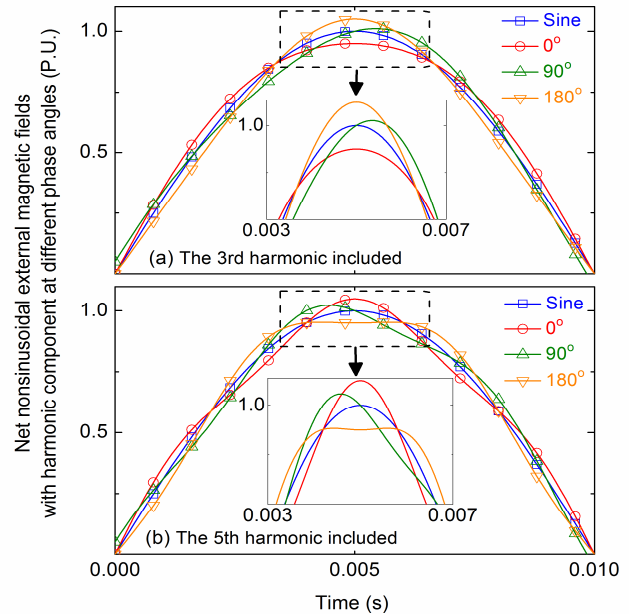


Fig. 1. Net external magnetic field waveform distorted by harmonics at $\varphi = \{0, 90^\circ, 180^\circ\}$, plotted together with sinusoidal external magnetic field. (a) The 3rd harmonic included (b) The 5th harmonic included

III. Harmonic magnetization AC loss: results and discussions

A 4-mm wide SuperPower tape was chosen to calculate the magnetization loss under distorted external magnetic fields. The main specifications of this tape are tabulated in Table I.

A. Effect of harmonic phase angle on magnetization AC losses

Fig. 1(a) and Fig. 1(b) illustrate the net external magnetic field per unit (P.U.) containing the 3rd and the 5th harmonics, respectively, at $\varphi_k = \{0, 90^\circ, 180^\circ\}$, compared with the pure sinusoidal magnetic field. In Fig. 1(a), the peak value of nonsinusoidal external magnetic field, A_{nemf} , has changed when φ_3 varies, and it follows $A_{\text{nemf}, \varphi_3=180} > A_{\text{nemf}, \varphi_3=90} > A_{\text{nemf}, \text{sine}} > A_{\text{nemf}, \varphi_3=0}$. In Fig. 1(b), there exists $A_{\text{nemf}, \varphi_5=0} > A_{\text{nemf}, \varphi_5=90} > A_{\text{nemf}, \text{sine}} > A_{\text{nemf}, \varphi_5=180}$.

Fig. 2(a) and Fig. 2(b) show the magnetization AC loss in HTS CC subjected to the external magnetic field which is distorted by the 3rd and the 5th harmonic, respectively, at $\text{THD} = 0.05$ and $B_1 = \{10, 20, 50, 100\}$ mT, plotted versus phase angle of harmonic magnetic field φ . It has been observed in both

Fig. 1(a)-(b) that, magnetization AC loss in HTS CC drastically increases with the increase of B_1 , at a fixed THD value.

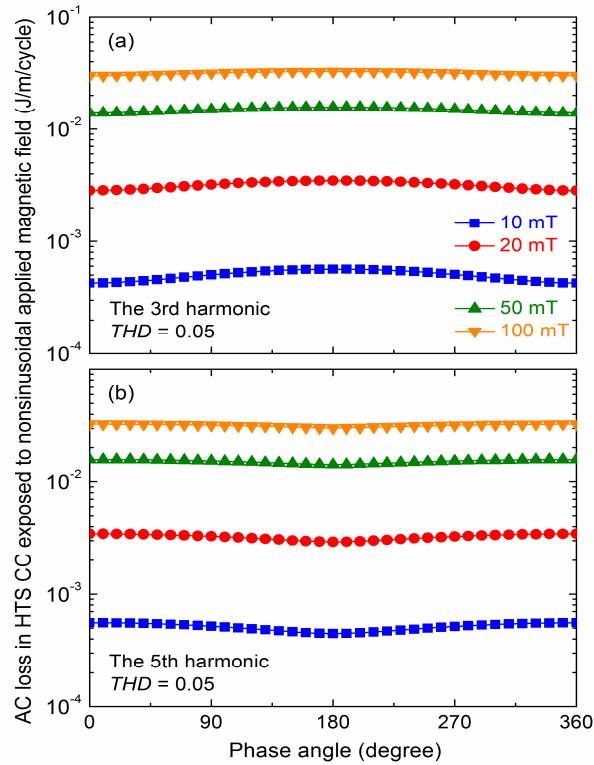


Fig. 2. Magnetization AC losses in HTS CC subjected to nonsinusoidal external magnetic field with different fundamental magnetic field amplitude, plotted against phase angle of field harmonics: the 3rd, and the 5th, at $THD_k = 0.05$.

Figs. 3(a)-(d) report calculated magnetization AC losses in HTS CC subjected to nonsinusoidal external magnetic field with the 3rd and the 5th harmonics, respectively, at $THD_k = 0.05$ for $B_1 = \{10, 20, 50, \text{ and } 100 \text{ mT}\}$, plotted against φ and compared with AC loss of sinusoidal external field, Q_{sine} . There are several phenomena observed from Fig. 3:

1) In Figs. 3(a)-(d), magnetization loss in HTS CC different φ_3 follows: $Q_{3rd, \varphi_3=180} > Q_{3rd, \varphi_3=90} > Q_{3rd, sine} > Q_{3rd, \varphi_3=0}$, which aligns well with the peak value of nonsinusoidal external magnetic field, A_{nemf} , as shown in Fig. 1(a). Similarly, magnetization loss in HTS CC at different φ_5 follows: $Q_{5th, \varphi_5=0} > Q_{5th, \varphi_5=90} \geq Q_{5th, sine} > Q_{5th, \varphi_5=180}$, which agrees with the peak value of nonsinusoidal external magnetic field, A_{nemf} , shown in Fig. 1(b). This is to say, magnetization AC loss under nonsinusoidal external magnetic field is dependent on the peak magnitude of the nonsinusoidal external magnetic field, A_{nemf} . As the magnetization loss is a hysteresis type loss.

2) When an HTS CC is exposed to nonsinusoidal external magnetic field with the 3rd harmonic (or the 5th harmonic) at a given B_1 , magnetization loss, Q_m changes at different φ value. When the 3rd harmonic was superimposed on the fundamental magnetic field, Q_m reaches the minimum at $\varphi_3 = 0^\circ$ and it reaches the maximum at $\varphi_3 = 180^\circ$. Q_m is higher than Q_{sine} when $80^\circ < \varphi_3 < 280^\circ$, while it is lower than Q_{sine} when $0^\circ < \varphi_3 < 80^\circ$, and $280^\circ < \varphi_3 < 360^\circ$. This is due to the fact that phase angle of 3rd harmonics changes the peak of the net external magnetic

field. However, when the 5th harmonic was superimposed on the fundamental magnetic field, Q_m reaches the minimum and

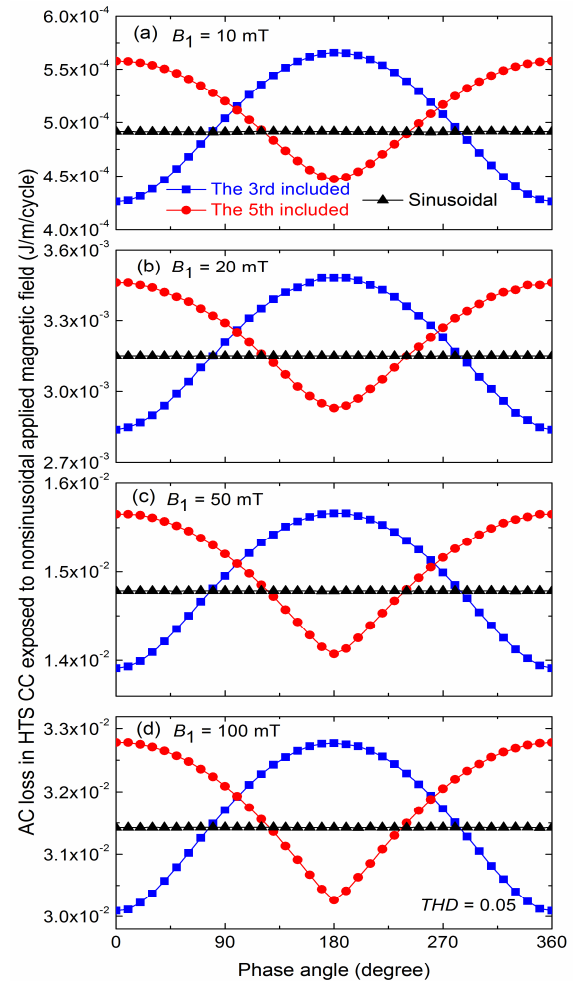


Fig. 3. Magnetization AC losses in HTS CC subjected to sinusoidal external field and nonsinusoidal external magnetic field with the 3rd, and the 5th harmonics at $THD_k = 0.05$ but different B_1 values, plotted against phase angle.

maximum value at $\varphi_5 = 180^\circ$ and $\varphi_5 = 0^\circ$, respectively. Q_m is higher than Q_{sine} when $0^\circ < \varphi_5 < 120^\circ$, and $240^\circ < \varphi_5 < 360^\circ$, while it is lower than Q_{sine} when $120^\circ < \varphi_5 < 240^\circ$.

3) It has been observed in Figs. 3(a)-(d) that, Q_m in HTS CC drastically increases with the increase of B_1 , at a fixed $THD = 0.05$. When B_1 increases from 10 to 100 mT, Q_m in HTS CC subjected to nonsinusoidal magnetic field with the 3rd harmonic increases by 110 times, and 85 times for the case of the 5th harmonic.

Fig. 4 and Fig. 5 plots and compares instantaneous losses in HTS CC exposed to the harmonics at lower and higher B_1 , 10 mT and 100 mT, respectively, at $\varphi_k = \{0^\circ, 90^\circ, 180^\circ\}$ and $THD_k = 0.05$. It is well known that AC loss is the integral of instantaneous loss over one period of applied external magnetic field. In Fig. 4, the maximum amplitude of instantaneous loss in case of the 5th harmonics are slightly higher than that of the 3rd harmonics. Two dominant peaks are observed in instantaneous loss profile resulted from distorted external magnetic field containing the 3rd harmonic, while there are three

dominant peaks in the 5th harmonic case.

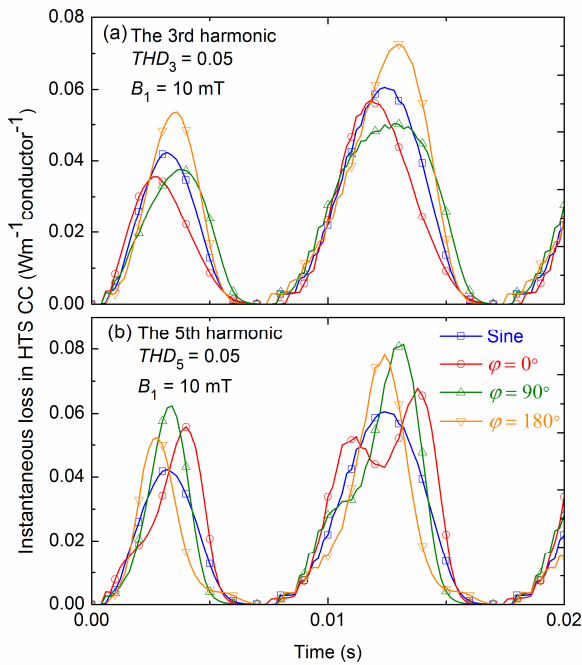


Fig. 4. Instantaneous loss in HTS CC subjected to nonsinusoidal external magnetic field at $B_1 = 10$ mT, $THD_k = 0.05$, and $\varphi = \{0, 90^\circ, 180^\circ\}$. (a) The 3rd harmonic included (b) The 5th harmonic included.

The maximum peak of instantaneous AC loss in case of the 3rd and the 5th harmonics belongs to $\varphi_3 = 180^\circ$ and $\varphi_5 = 90^\circ$; but the integration of instantaneous AC loss in one period is the highest at $\varphi_3 = 180^\circ$ and $\varphi_5 = 0^\circ$ for 3rd and 5th harmonics, respectively.

In Fig. 5, the amplitude of peaks of instantaneous loss has substantial improvement when B_1 rises from 10 mT from 100 mT. The peaks are slightly higher for the 5th harmonics compared with the 3rd harmonic. At higher external magnetic field, the peak at $\varphi = 0^\circ$ is always higher than others in both the 3rd and the 5th harmonic cases. But the integral of instantaneous loss (area under curve) reaches the maximum for the 3rd harmonic when $\varphi = 180^\circ$, and for 5th harmonic when $\varphi = 0^\circ$.

B. Effect of THD on harmonic magnetization AC losses

Fig. 6(a) and Fig. 6(b) plot J/J_c distribution along the width of an HTS CC which is exposed to nonsinusoidal external magnetic field with the 3rd and 5th harmonics, respectively, at $B_1 = 10$ mT and $THD = \{0.05, 0.2\}$. In Fig. 6(a), a bigger penetration depth was found at $\varphi_3 = 180^\circ$ than $\varphi_3 = 0^\circ$, both at $THD_3 = 0.05$ and 0.2. This is consistent with AC loss behavior shown in Fig. 3 that minimum and maximum Q_m occurs at $\varphi_3 = 0^\circ$ and 180° . While at a given φ_3 value, more J is penetrated in HTS CC at $THD_3 = 0.2$, compared to $THD_3 = 0.05$.

In Fig. 6(b), there is less J penetrated into the HTS CC at $\varphi_5 = 180^\circ$ than $\varphi_5 = 0^\circ$, both at $THD_5 = 0.05$ and 0.2. This is also in agreement with AC loss behavior shown in Fig. 3. At a given φ_5 value, more J is penetrated in HTS CC at $THD_3 = 0.2$, compared to $THD_3 = 0.05$.

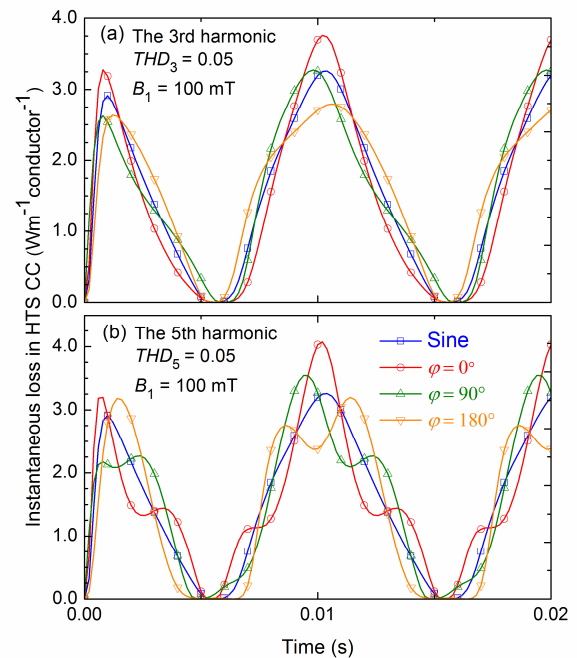


Fig. 5. Instantaneous loss in HTS CC subjected to nonsinusoidal external magnetic field at $B_1 = 100$ mT, $THD_k = 0.05$, and $\varphi = \{0, 90^\circ, 180^\circ\}$. (a) The 3rd harmonic included (b) The 5th harmonic included.

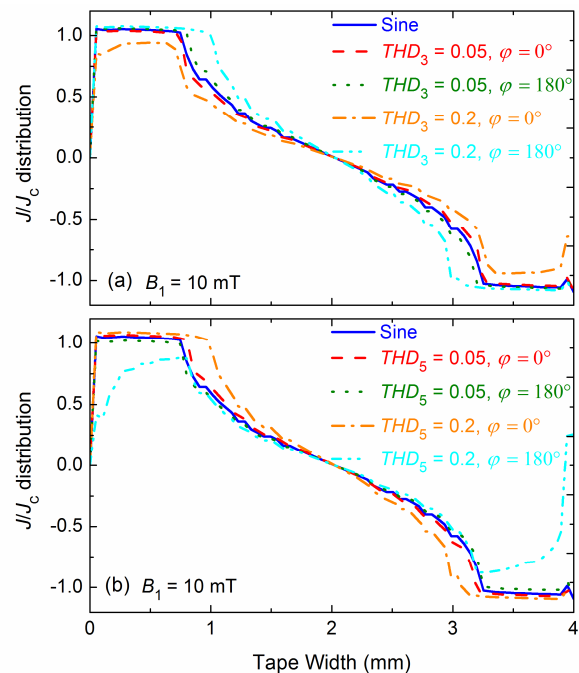


Fig. 6. J/J_c distribution along the width of HTS CC exposed to nonsinusoidal external magnetic field at $B_1 = 10$ mT and different THD level. (a) The 3rd harmonic included (b) The 5th harmonic included.

Fig. 7(a) and 7(b) report magnetization AC losses in HTS CC exposed to nonsinusoidal magnetic field with the 3rd and the 5th harmonics included, respectively, at fixed $B_1 = 10$ mT but different THD_k values ranging from 0.02 to 0.2, plotted against Q_{sine} . Some phenomena/findings were found in Fig. 7:

1) AC loss in HTS CC exposed to nonsinusoidal magnetic field with the 3rd harmonic always reach the minimum

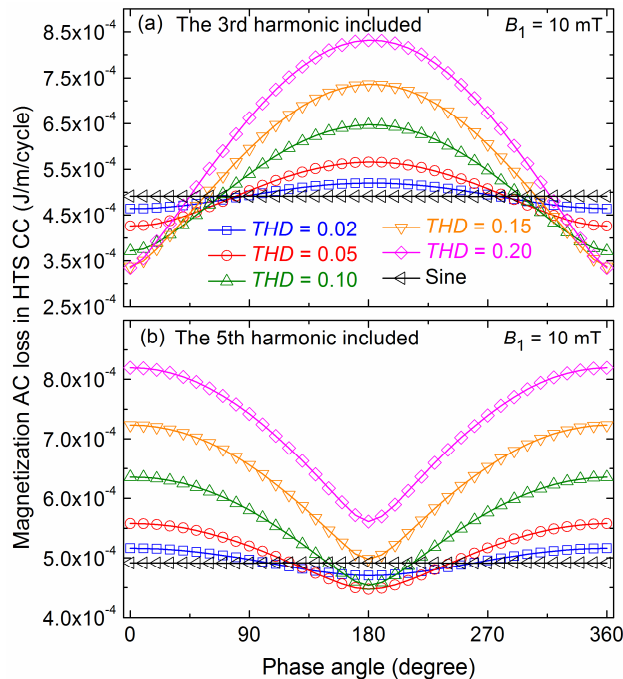


Fig. 7. Magnetization AC losses in HTS CC subjected to nonsinusoidal external magnetic field with harmonics at $B_1 = 10$ mT but different THD_k values ranging from 0.02 to 0.2, plotted against phase angle of magnetic field harmonics. (a) The 3rd harmonic included (b) The 5th harmonic included

at $\varphi_3 = 0^\circ$ and the maximum at $\varphi_3 = 180^\circ$, at different THD values and $B_1 = 10$ mT. AC loss in HTS CC exposed to nonsinusoidal magnetic field with the 5th harmonic always reach the minimum at $\varphi_3 = 180^\circ$ and the maximum at $\varphi_5 = 0^\circ$, at different THD values and $B_1 = 10$ mT.

2) $Q_{3rd, \varphi_3 = 0}$ and $Q_{3rd, \varphi_3 = 180}$ are THD level dependent, i.e., $Q_{3rd, \varphi_3 = 0}$ reduces with the increase of THD and $Q_{3rd, \varphi_3 = 180}$ increases with the increase of THD, when THD varies from 0.02 to 0.2. On the other hand, $Q_{5th, \varphi_5 = 0}$ and $Q_{5th, \varphi_5 = 180}$ are THD level dependent too, i.e., $Q_{5th, \varphi_5 = 0}$ increases with the increase of THD and $Q_{5th, \varphi_5 = 180}$ reduces with the increase of THD, when THD varies from 0.02 to 0.2.

Fig. 8 reports the instantaneous loss of tape exposed to external magnetic field with the 3rd and the 5th harmonics at $THD = 0.2$ and $B_1 = 100$ mT. The amplitude of peaks of instantaneous AC loss have been increased as compared to those in Fig. 4 when $THD = 0.05$ and $B_1 = 100$ mT. However, the number of peaks in instantaneous loss distorted by the 5th harmonic is more obvious in $THD = 0.2$, as compared with $THD = 0.05$. Another interesting observation is that the number of peaks in $THD_5 = 0.2$ is higher than $THD_5 = 0.05$. It is because of higher fluctuation and distortion caused by the 5th harmonics.

C. Effect of n-value and B-dependency of critical current density on harmonic magnetization AC losses

As shown in Fig. 9, calculated magnetization losses of a single coated conductor get slightly increased around 2.1% when n value decreases from 30 to 20, at $THD_5 = 10\%$, $B_1 = 20$ mT, and any phase angle. This is due to the fact that with a larger n value, the E-J curve get steeper, approaching to CS model. Actually, n value, as a good indicator of the E-I resistive transition, shows that a larger

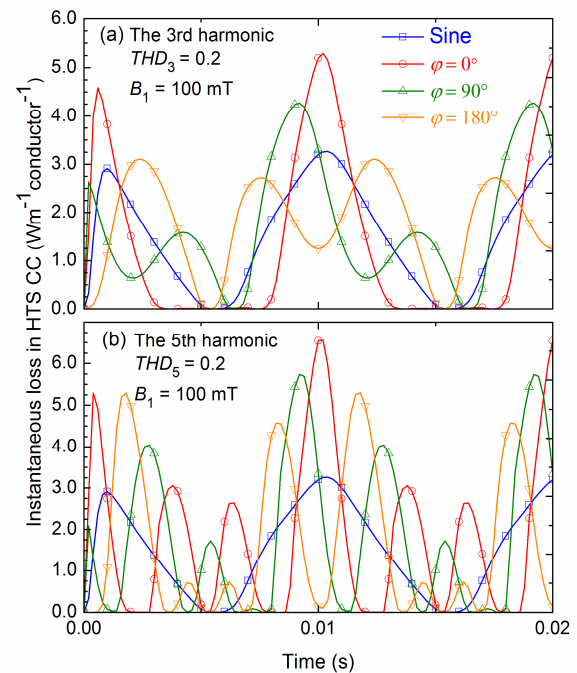


Fig. 8. Instantaneous loss in HTS CC subjected to nonsinusoidal external magnetic field at $B_1 = 100$ mT, $THD_k = 0.2$, and $\varphi = \{0, 90^\circ, 180^\circ\}$. (a) The 3rd harmonic included (b) The 5th harmonic included.

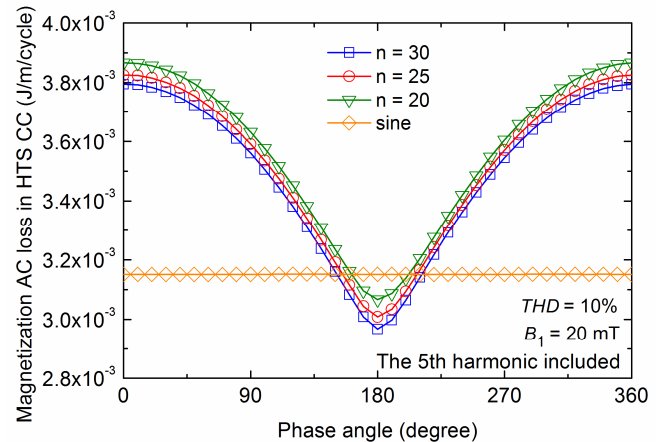


Fig. 9. Magnetization loss of superconductor when exposed to external magnetic field at $B_y = 20$ mT, $THD_5 = 10\%$, and varying n values

n value indicates the improvement of I_c of the superconductor, which leads to slightly lower AC losses [32].

In order to demonstrate the $J_c(B)$ dependence on the nonsinusoidal AC losses, we carried out another calculation with constant $J_c = J_{c0}$, the self-field critical current density. The case study was chosen at $B_1 = 20$ mT, $THD_5 = 10\%$. In Fig. 10, magnetization loss of a single coated conductor calculated by considering $J_c(B)$ is always larger than that calculated by considering constant J_c , at $B_1 = 20$ mT, $THD_5 = 10\%$ and any phase angle. It is roughly estimated that the effective penetration field of the superconductor at self-field 77 K is 21.2 mT. When the $J_c(B)$ effect is considered, J_c under external magnetic field will be degraded and thus, the penetration field

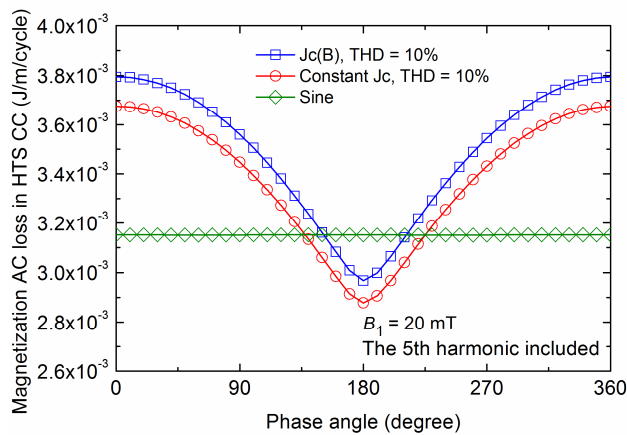


Fig. 10. Magnetization loss of superconductor when exposed to external magnetic field at $B_1 = 20$ mT, 5rd, THD = 10%.

will decrease, accordingly. In this case study, we chose 20 mT as the external magnetic field, which is smaller than the penetration field calculated by self-field J_c [33]. Therefore, when constant J_c is considered in the calculation, magnetization loss would be underestimated.

IV. Conclusion

In this paper, we carried out a series of numerical calculations to study the nonsinusoidal magnetization loss in HTS CC exposed to external magnetic field polluted with the 3rd and the 5th harmonic components, at various harmonic phase angles φ ranging from 0° to 360° and different amplitude of fundamental magnetic field B_1 , and harmonic distortion level, denoted by THD, was chosen to be 0 to 0.2.

Magnetization loss in HTS CC under nonsinusoidal magnetic field with the 3rd harmonic meets the minimum and maximum at $\varphi_3 = 0^\circ$ and $\varphi_3 = 180^\circ$, respectively, at a fixed B_1 and THD value. On the contrary, magnetization loss in HTS CC under nonsinusoidal magnetic field with the 5th harmonic reaches the minimum and maximum at $\varphi_5 = 180^\circ$ and $\varphi_5 = 0^\circ$, respectively. This is due to the compensation effect of magnetic field waveforms and the maximum peak of resultant nonsinusoidal magnetic field waveforms roughly dominates the AC loss.

Magnetization loss in HTS CC under external magnetic field with the 3rd or the 5th harmonic drastically increases with the increase of B_1 , at a fixed THD in the range of 0 to 0.2 and a fixed phase angle in the range of 0° to 360° , due to deeper magnetic field penetration in HTS CC.

At a fixed B_1 and phase angle, magnetization loss in HTS CC under external magnetic field with the 3rd or the 5th harmonic increases proportionally with the increase of THD.

V. References

[1] K. S. Haran, S. Kalsi, T. Arndt, H. Karmaker, R. Badcock, B. Buckley, T. Haugan, M. Izumi, D. Loder, J. W. Bray, P. Masson, and E. W. Stautner, "High Power Density Superconducting Machines – Development Status and Technology Roadmap", *Superconductor Science and Technology*, vol. 30, no. 12, pp. 1-30, 2017.

[2] M. Yazdani-Asrami, M. Zhang, and W. Yuan, "Challenges for developing high temperature superconducting ring magnets for rotating electric machine applications in future electric aircrafts," *Journal of Magnetism and Magnetic Materials*, vol. 522, pp. 1-3, 2021.

[3] Y. Wang, C. Wan Kan, and J. Schwartz, "Self-protection mechanisms in no-insulation (RE)Ba 2Cu 3O x high temperature superconductor pancake coils," *Superconductor Science and Technology*, vol. 29, no. 4, pp. 045007, April 2016.

[4] W. Song, Z. Jiang, M. Staines, R. A. Badcock, S. C. Wimbush, J. Fang, and J. Zhang, "Design of a single-phase 6.5 MVA/25 kV superconducting traction transformer for the Chinese Fuxing high-speed train," *International Journal of Electrical Power & Energy Systems*, vol. 119, Art. no. 105956, 2020.

[5] B. Liu, S. Wang, B. Zhao, X. Wang, and J. Fang, "Research on AC losses of racetrack superconducting coils applied to high-temperature superconducting motors", *Superconductor Science and Technology*, vol. 32, no. 1, pp. 1-11, 2019.

[6] B. Liu, R. Badcock, H. Shu, L. Tan, and J. Fang, "Electromagnetic Characteristic Analysis and Optimization Design of a Novel HTS Coreless Induction Motor For High-Speed Operation", *IEEE Transactions on Applied Superconductivity*, vol. 28, no. 4, pp. 1-5, 2018.

[7] R. M. Scanlan, A. P. Malozemoff, and D. C. Larbalestier, "Superconducting materials for large scale applications," *Proceedings of the IEEE*, vol. 92, no. 10, pp. 1639-1654, 2004.

[8] W. Zhou, Z. Jiang, M. Staines, W. Song, C. W. Bumby, R. A. Badcock, N. J. Long, and J. Fang, "Magnetization Loss in REBCO Roebel Cables with Varying Strand Numbers," *IEEE Transactions on Applied Superconductivity*, vol. 28, no. 3, pp. 1-5, 2018.

[9] M. Yazdani-Asrami, M. Mirzaie, and A. Akmal, "No-load loss calculation of distribution transformers supplied by nonsinusoidal voltage using three dimensional finite element analysis," *Energy*, vol. 50, pp. 205-219, 2013.

[10] M. Yazdani-Asrami, S. A. Gholamian, S. M. Mirimani, and J. Adabi, "Calculation of AC Magnetizing Loss of ReBCO Superconducting Tapes Subjected to Applied Distorted Magnetic Fields", *Journal of Superconductivity and Novel Magnetism*, vol. 31, no.12, pp. 3875-3888, 2018.

[11] R. Kulkarni, K. Prasad, T. Tjing Lie, R. A. Badcock, C. W. Bumby, and H. J. Sung, "Design Improvisation for Reduced Harmonic Distortion in a Flux Pump-Integrated HTS Generator," *Energies*, vol. 10, no. 9, pp. 1-14, 2017.

[12] G. J. Wakileh, "Harmonics in rotating machines," *Electric Power Systems Research*, vol. 66, no. 1, pp. 31-37, 2003.

[13] B. Douinc, J. Leveque, A. Rezzoug, "AC loss Measurements of a High Critical Temperature Superconductor Transporting Sinusoidal or Nonsinusoidal Current," *IEEE Transactions in Applied Superconductivity*, vol. 10, no. 1, pp. 1489-1492, 2000.

[14] F. Grilli, E. Pardo, A. Stenvall, D. N. Nguyen, W. Yuan, and F. Gomory, "Computation of Losses in HTS Under the Action of Varying Magnetic Fields and Currents", *IEEE Transactions on Applied Superconductivity*, vol. 24, no. 1, pp. 1-33, 2014.

[15] M. Chudy, Y. Chen, M. Zhang, M. Baghdadi, J. Lalk, T. Pretorius, and T. Coombs, "Power Losses of 2G HTS Coils Measured in External Magnetic DC and Ripple Fields", *IEEE Transactions on Applied Superconductivity*, vol. 24, no. 1, pp. 1-6, 2014.

[16] V. Sokolovsky, V. Meerovich, M. Spektor, G. A. Levin, and I. Vajda, "Losses in Superconductors under Non-Sinusoidal Currents and Magnetic Fields", *IEEE Transactions on Applied Superconductivity*, vol. 19, no. 3, pp. 3344-3347, 2009.

[17] G. Furman, M. Spektor, V. Meerovich, and V. Sokolovsky, "Losses in coated conductors under non-sinusoidal currents and magnetic fields", *Journal of Superconductivity and Novel Magnetism*, vol. 24, no.1-2, pp. 1045-1051, 2011.

[18] M. Vojenciak, J. Souc, J. M. Ceballos, F. Gomory, B. Klincok, E. Pardo, and F. Grilli, "Study of ac loss in Bi-2223/Ag tape under the simultaneous action of ac transport current and ac magnetic field shifted in phase", *Superconductor Science and Technology*, vol. 19, no. 4, pp. 397-404, 2006.

[19] B. Shen, C. Li, J. Geng, X. Zhang, J. Gawith, J. Ma, Y. Liu, F. Grilli, and T. A. Coombs, "Power dissipation in HTS coated conductor coils under the simultaneous action of AC and DC currents and fields," *Superconductor Science and Technology*, vol. 31, no. 7, pp. 1-12, 2018.

[20] B. Shen, C. Li, J. Geng, Q. Dong, J. Ma, J. Gawith, K. Zhang, Z. Li, J. Chen, W. Zhou, X. Li, J. Sheng, Z. Li, Z. Huang, J. Yang, and T. A. Coombs, "Power Dissipation in the HTS Coated Conductor Tapes and Coils Under the Action of Different Oscillating Currents and Fields," *IEEE Transactions in Applied Superconductivity*, vol. 29, no. 5, pp. 1-5, 2019.

[21] M. Yazdani-Asrami, S. A. Gholamian, S. M. Mirimani, and J. Adabi, "Influence of Field-Dependent Critical Current on Harmonic AC Loss Analysis in HTS Coils for Superconducting Transformers Supplying Non-Linear Loads", *Cryogenics*, Early access, 2021.

[22] M. Yazdani-Asrami, W. Song, M. Zhang, W. Yuan, and X. Pei, "AC Transport Loss in Superconductors Carrying Harmonic Current With Different

Phase Angles for Large-Scale Power Components,” *IEEE Transactions in Applied Superconductivity*, vol. 31, no. 1, pp. 1–5, 2021.

[23] M. Yazdani-Asrami, M. Taghipour-Gorjikolaie, W. Song, M. Zhang, and W. Yuan, “Prediction of nonsinusoidal AC loss of superconducting tapes using artificial intelligence-based models,” *IEEE Access*, vol. 8, pp. 207287–207297, 2020.

[24] Z. Hong, A. M. Campbell, and T. A. Coombs, “Numerical solution of critical state in superconductivity by finite element software,” *Superconductor Science and Technology*, vol. 19, pp. 1246–1252, 2006.

[25] R. Brambilla, F. Grilli, and L. Martini, “Development of an edge-element model for AC loss computation of high-temperature superconductors,” *Superconductor Science and Technology*, vol. 20, pp. 16–24, 2006.

[26] V. M. R. Zermeno, N. Mijatovic, C. Træholt, T. Zirngibl, E. Seiler, A. B. Abrahamsen, N. F. Pedersen, and M. P. Sorensen, “Towards faster FEM simulation of thin film superconductors: a multiscale approach,” *IEEE Transactions in Applied Superconductivity*, vol. 21, pp. 3273–3276, 2011.

[27] W. Song, Z. Jiang, X. Zhang, M. Staines, R. Badcock, J. Fang, Y. Sogabe, and N. Amemiya, “AC loss simulation in a HTS 3-Phase 1 MVA transformer using H formulation,” *Cryogenics*, vol. 94, pp. 14–21, 2018.

[28] M. Yazdani-Asrami, S. A. Gholamian, S. M. Mirimani, and J. Adabi, “Investigation on Effect of Magnetic Field Dependency Coefficient of Critical Current Density on the AC Magnetizing Loss in HTS Tapes Exposed to External Field”, *Journal of Superconductivity and Novel Magnetism*, vol. 31, no.12, pp. 3899–3910, 2018.

[29] S. Li, D. X. Chen, and J. Fang, Transport ac losses of a second-generation HTS tape with a ferromagnetic substrate and conducting stabilizer, *Superconductor Science and Technology*, vol. 28, no. 12, pp.125011, 2015.

[30] W. Song, J. Fang, and Z. Jiang, “Numerical AC Loss Analysis in HTS Stack Carrying Non-sinusoidal Transport Current,” *IEEE Transactions in Applied Superconductivity*, vol. 29, no. 2, pp. 1–5, 2019.

[31] M. Yazdani-Asrami, W. Song, X. Pei, M. Zhang, and W. Yuan, “AC Loss Characterization of HTS Pancake and Solenoid Coils Carrying Nonsinusoidal Currents,” *IEEE Transactions in Applied Superconductivity*, vol. 30, no. 5, pp. 1–9, 2020.

[32] S. Li, and D. X. Chen, Scaling law for voltage–current curve of a superconductor tape with a power-law dependence of electric field on a magnetic-field-dependent sheet current density, *Physica C*, vol. 538, 2017, pp. 32–39.

[33] Y. Liu, Z. Jiang, Q. Li, C. W. Bumby, R. A. Badcock, and J. Fang, “Dynamic resistance measurement in a four-tape YBCO stack with various applied field orientation,” *IEEE Transactions on Applied Superconductivity*, vol. 29, no. 5, pp. 1–7, 2019.



Mohammad Yazdani-Asrami (Member, IEEE) received his Ph.D. degree in Electrical Power Engineering at early 2018. He was a visiting researcher/research assistant on a superconducting machine project at Superconductivity Division of ENEA, Frascati, Italy at 2015. He also worked as research assistant on a project for design development and fabrication of a fault tolerant superconducting transformer at Robnson Research Institute, Victoria University of Wellington, New Zealand from 2016 to 2017. He also worked as project engineer for testing electric machine and components at University of Warwick, United Kingdom.

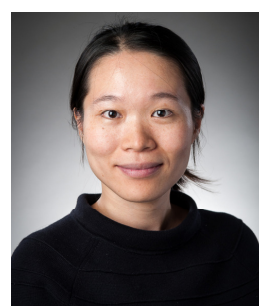
He is currently a postdoctoral research associate at the department of electronic and electrical engineering, University of Strathclyde, Glasgow, United Kingdom. His field of expertise and interest is applied superconductivity for large-scale power applications, Cryoelectrification for modern transportation systems, material characterization as well as AC loss calculation and measurement for HTS and MgB₂ tapes and wires, and design development of superconducting rotating machine, transformers, fault current limiters, and cables.



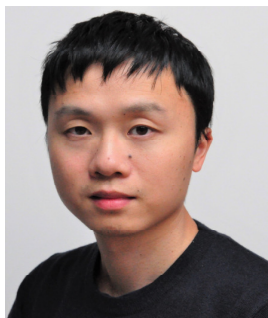
Wenjuan Song (Member, IEEE) received the M.Eng and the Ph.D. degrees in Electrical Engineering from Beijing Jiaotong University (BJTU), China, in 2015 and 2019, respectively.

She was a visiting researcher/research assistant in Robnson Research Institute, Victoria University of Wellington, New Zealand for more than two years from 2016 to 2018. Since 2019, she joined as a postdoctoral research associate in department of electronic & electrical engineering at University of Bath.

Her field of expertise is electromagnetic analysis for superconducting power applications, AC loss calculation and measurement of superconductors, design and development of superconducting fault current limiters and transformers.



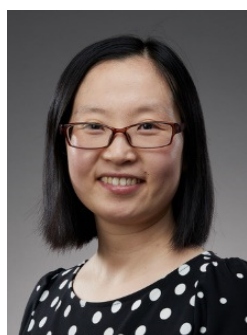
Min Zhang (Member, IEEE) received her PhD from the University of Cambridge in Engineering. Before that, she received Bachelor and Master degrees from Tsinghua University in Electrical Engineering. Dr Zhang spent a year as a Junior Research Fellow at Newnham College, Cambridge and then joined University of Bath as a Lecturer. She joined the University of Strathclyde as a Reader in 2018 and is currently a Research Fellow of Royal Academy of Engineering. Dr Zhang’s research focuses on the application of high temperature superconductors in power system transmission, renewable generation and electric transportation.



Weijia Yuan (Senior Member, IEEE) received his Bachelor degree from Tsinghua University in 2006 and his PhD from the University of Cambridge in 2010. He then became both a research associate in the Engineering Department and a junior research fellow at Wolfson College, both at the University of Cambridge from 2010 to 2011. Dr Yuan joined the University of Bath as a Lecturer/Assistant Professor in 2011, where he was later promoted to

Reader/Associate Professor in 2016. He joined the University of Strathclyde as a Professor in 2018.

He is now leading a research team in the area applied superconductivity including energy storage, fault current limiters, machines and power transmission lines. He has been working closely with industry partners on all electric propulsion for future electric aircraft, designing a fully superconducting system for aerospace application. His work also involves renewable energy integration and power system stability using energy storage systems.



Xiaoze Pei (Member, IEEE) received the B.Eng. and M.Eng. degrees from Beijing Jiaotong University, Beijing, China in 2006 and 2008, respectively. She received the Ph.D. degree from the University of Manchester, Manchester, U.K. in 2012. She became a Research Associate at the University of Manchester. In 2017, she joined the University of Bath as a Lecturer.

She has extensive research experience in designing and building of superconducting fault current limiters and fast operating vacuum circuit breakers. Her research interests include electrical power applications of superconductivity and hybrid DC circuit breaker.